International Journal of Modern Physics E
Vol. 19, Nos. 8 & 9 (2010) 1794–1801
© World Scientific Publishing Company
DOI: 10.1142/S0218301310016223

World Scientific
www.worldscientific.com

THE ORIENTATIONAL-AVERAGE EFFECTS OF HEAVY-ION COLLISIONS INDUCED BY DEFORMED NUCLEI AT INTERMEDIATE ENERGY

X. G. CAO[1,2], X. Z. CAI[1,*], G. Q. ZHANG[1,2], Y. G. MA[1], J. G. CHEN[1], D. Q. FANG[1], W. GUO[1], G. H. LIU[1], W. D. TIAN[1] and H. W. WANG[1]

[1]*Shanghai Institute of Applied Physics, Chinese Academy of Sciences, Shanghai 201800, China*
[2]*Graduate School of the Chinese Academy of Sciences, Beijing 100080, China*
[*]*caixz@sinap.ac.cn*

The deformed projectiles and targets are expected to play different roles in heavy-ion collisions (HICs) at intermediate energy compared with spherical ones. With an isospin-dependent quantum molecular dynamics (IDQMD) model, in despite of averaging all the orientations of axisymmetric deformed ^{24}Mg + ^{24}Mg collisions, it is still found that NN collision number, nuclear stopping power (R) and multiplicity of fragments have considerable differences compared with spherical ^{24}Mg + ^{24}Mg collisions.

1. Introduction

Nuclear reactions involving the deformed projects and targets have been studies several decades ago.[1,2] In heavy-ion collisions, the deformation and orientation also affect reaction cross section,[3] elliptic flow[4] and heavy-ion fusion.[5,6] In addition, the U + U collisions is proposed as a more promising scheme to study quark-gluon plasma (QGP) at relativistic and ultrarelativistic energies recently.[7–14] Nuclei far from β-stability line with large deformation become available due to the recent development of radioactive beam facilities. Thus it is necessary to consider the deformed effects of the projectile and target in HICs. However, the knowledge about the deformed nuclei collisions is very poor at intermediate energy. On the other hand, highly deformed nuclei induced reactions may inspire the exotic nuclei research such as the halo[15] and cluster phenomena.[16]

In this paper, using IDQMD model, the average effects of deformation and orientation are studied by axisymmetric deformed ^{24}Mg + ^{24}Mg collisions with incident energy from 15 to 520MeV/nucleon. ^{24}Mg is approximately treated as a sharp-cutoff ellipsoid with large quadrupole deformation parameter: $\beta_2 = 0.416$ getting from relativistic mean field calculation.[17] The spherical ^{24}Mg + ^{24}Mg collisions with the same root mean-square radius are used for comparison.

The rest of the paper is organized as follows: Sec. 2 gives a brief introduction of the IDQMD model. In Sec. 3, the calculated results such as: binary collision num-

ber, nuclear stopping power, multiplicity of fragments are compared with spherical ^{24}Mg + ^{24}Mg collisions. A summary is given in Sec. 4.

2. Description of the IDQMD Model

The quantum molecular dynamics (QMD) approach is a many-body theory that can describe HICs from intermediate to relativistic energies.[18,19] The main advantage of the QMD model is that it can explicitly treat the many body state of the collision system, so it contains correlation effects to all orders. Therefore, the QMD model provides valuable information about both the collision dynamics and the fragmentation process. The model also has excellent extensibility due to it's microscopic treatment of collision process. It includes several important parts: initialization of the projectile and the target nucleons, propagation of nucleons in the effective potential, NN collisions in a nuclear medium, the Pauli blocking and the numerical test.

The IDQMD model is based on QMD model and affiliates the isospin factors in mean field, two-body NN collisions and Pauli blocking.[20–22] In addition, the phase space sampling of neutrons and protons in the initialization should be treated separately because of the large differences between neutron and proton density distributions for nuclei far from the β-stability line.

In IDQMD model, each nucleon is represented by a Gaussian wave packet with a width $\sqrt{L}$ (here $L = 2.16$ fm^2) centered around the mean position $\mathbf{r_i}(t)$ and the mean momentum $\mathbf{p_i}(t)$,

$$\psi_i(\mathbf{r},t) = \frac{1}{(2\pi L)^{3/4}} \exp\left[-\frac{(\mathbf{r}-\mathbf{r_i}(t))^2}{4L}\right] \exp\left[\frac{i\mathbf{r}\cdot\mathbf{p_i}(t)}{\hbar}\right]. \tag{1}$$

The nuclear mean field is parameterized by

$$U(\rho,\tau_z) = \alpha\left(\frac{\rho}{\rho_0}\right) + \beta\left(\frac{\rho}{\rho_0}\right)^{\gamma} + \frac{1}{2}(1-\tau_z)V_c + C_{\rm sym}\frac{\rho_n-\rho_p}{\rho_0}\tau_z + U^{\rm Yuk}. \tag{2}$$

with $\rho_0 = 0.16$ fm^{-3} (the normal nuclear matter density). ρ, ρ_n and ρ_p are the total, neutron and proton densities, respectively. τ_z is zth component of the isospin degree of freedom, which equals 1 or -1 for neutrons or protons, respectively. The coefficients α, β and γ are parameters of nuclear equation of state (EOS). C_{sym} is the symmetry energy strength due to the difference of neutron and proton. In this work, $\alpha = -356$ MeV, $\beta = 303$ MeV and $\gamma = 7/6$ are taken which corresponds to the so-called soft EOS with an incompressibility of $K = 200$ MeV and $C_{sym} = 32$ MeV.[19] V_c is the Coulomb potential and U^{Yuk} is Yukawa (surface) potential, which

has the following form:

$$U^{\rm Yuk} = \frac{V_y}{2m}\sum_{i\neq j}\frac{1}{r_{ij}}\exp(Lm^2) \times [\exp(-mr_{ij})erf(\sqrt{L}m - r_{ij}/\sqrt{4L}) - \exp(mr_{ij})erf(\sqrt{L}m + r_{ij}/\sqrt{4L})]. \quad (3)$$

with $V_y = 0.0074$ GeV, $m = 1.25\ fm^{-1}$, $L = 2.16\ fm^2$ and $r_{ij} = |\mathbf{r_i} - \mathbf{r_j}|$ is the relative distance between two nucleons. Experimental parameterized NN cross section which is energy and isospin dependent is used.

The Pauli blocking effect in IDQMD model is also isospin dependent and the blocking of neutron and proton is separate as following: each nucleon occupies a six-dimensional sphere with a volume of $\hbar^3/2$ in the phase space (considering the spin degree of freedom) and we calculate the phase volume (V) of the scattered nucleons being occupied by the rest nucleons with the same isospin as that of the scattered ones. We then compare $2V/\hbar^3$ with a random number and decide whether the collision is blocked or not.

In the present work, The ^{24}Mg nucleons' coordinates are initialized by sampling from a sharp-cutoff uniform ellipsoid with deformation parameters given above to incorporate initial nuclear deformed effects into the microscopic transport process. The long and short semiaxis of the ellipsoid take the following values:

$$R_l = R\cdot\left(1+\frac{2}{3}\delta_D\right). \quad (4)$$

$$R_s = R\cdot\left(1-\frac{1}{3}\delta_D\right). \quad (5)$$

where R is the radius of an equivalent spherical volume with the ellipsoid and

$$\delta_D = \frac{3}{2}\sqrt{\frac{5}{4\pi}}\beta_2. \quad (6)$$

For $\beta_2 = 0.416$, $R_l = 4.8\ fm$, $R_s = 3.3\ fm$ and R=3.9 fm. Then the momentum distribution of nucleons is generated by means of the local Fermi gas approximation:

$$P_F^i(\mathbf{r}) = \hbar[\mathbf{3}\pi^{\mathbf{2}}\rho_{\mathbf{i}}(\mathbf{r})]^{\mathbf{1/3}},\quad (\mathbf{i} = \mathbf{n}, \mathbf{p})\,. \quad (7)$$

The stability of the initialized nuclei are checked by time evolution till 200fm/c according to the average binding energies and root mean-square radii of the system at zero temperature. Only the initialized nuclei whose average binding energies and root mean-square radii meet the required values are stored to simulate the collisions. The distributions of coordinate space of stable ^{24}Mg with $\beta_2 = 0.416$ is show in Fig. 1.

The time evolution of the colliding system is given by the generalized variational principle. Since the QMD can naturally include the fluctuation and correlation, we

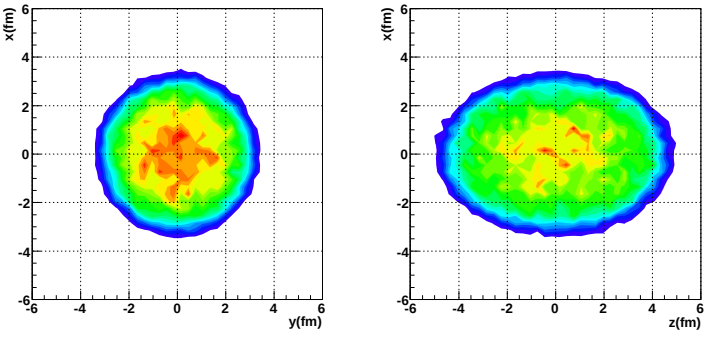

Fig. 1. (Color online) The projection of initial nucleons in coordinate space of stable ^{24}Mg with $\beta_2 = 0.416$ in the initialization of IDQMD calculations.

can study the different fragmentation processes due to the different shapes of reaction sources. In QMD model, nuclear clusters are constructed by a coalescence model, in which nucleons with relative momentum smaller than P_0 and relative distance smaller than R_0 are considered to belong one cluster. We adopt the parameter set: $P_0 = 300$ MeV/c and $R_0 = 3.5$ fm.

3. Calculated Results and Discussions

The differences between orientational-average deformed and spherical ^{24}Mg + ^{24}Mg are discussed in three aspects: the number of NN collisions, nuclear stopping power and distributions of fragments. Nuclear stopping power and fragments observables are extracted at freeze-out time (200 fm/c).

3.1. *Binary collisions*

From the model introduced above, we know that NN collision plays a very important role in intermediate energy reactions. Different overlaps of deformed and spherical collisions will lead to different collisions processes. Fig. 2 gives the impact parameter dependence of NN collision number for deformed and spherical ^{24}Mg + ^{24}Mg collisions at several incident energies. Spherical configuration has more NN collisions especially for lower incident energies. This partly contributes to differences in nuclear stopping and fragments distributions.

3.2. *Nuclear stopping power*

The nuclear stopping power (R) is defined by

$$R = \frac{2}{\pi} \frac{\sum_i^A \mid P_{i\perp} \mid}{\sum_i^A \mid P_{i\parallel} \mid}, \tag{8}$$

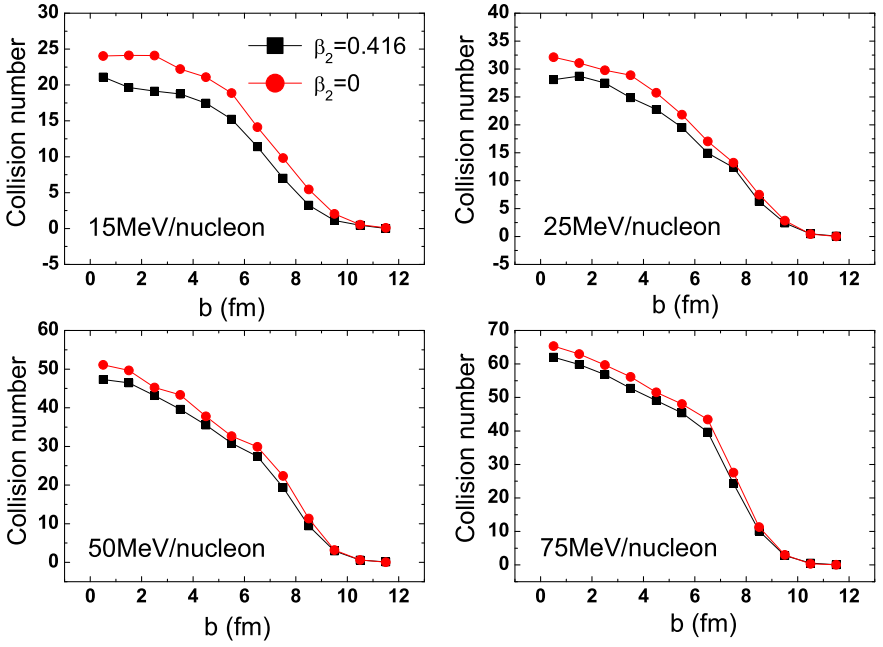

Fig. 2. (Color online) Binary collision number as a function of impact parameter at freeze-out time for deformed and spherical ^{24}Mg + ^{24}Mg collisions at different incident energies.

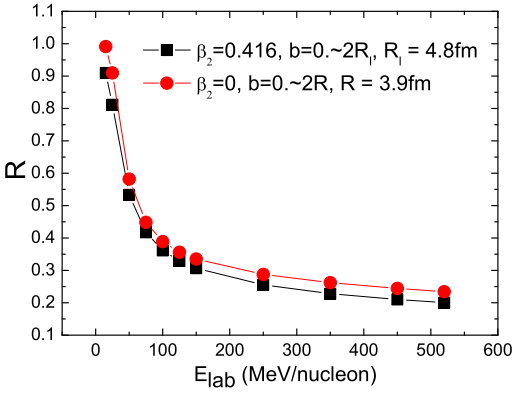

Fig. 3. (Color online) Nuclear stopping power as a function of incident energy at freeze-out time for deformed and spherical ^{24}Mg + ^{24}Mg collisions.

with A refers to the sum of projectile mass number and target mass number, $P_{i\perp} = (P_{ix}^2 + P_{iy}^2)^{1/2}$, $P_{i\parallel} = P_{iz}$ in the c.m. reference system, which measures the degree of isotropy of nucleons' momentum based on event-by-event. Thus, R can be used to

describe the momentum dissipation and the degree of thermalization. As R equals unity, isotropy of momentum is reached, which is not sufficient but necessary for thermalization equilibrium of the collision system.[23] Nuclear stopping power can be used to reflect the global property of HICs. Fig. 3 shows R of deformed and spherical ^{24}Mg + ^{24}Mg collisions. The differences of R become larger at higher incident energies.

3.3. *Fragments observables*

One of the main advantages of QMD model is that it can naturally treat the formation of fragments. The multiplicity of fragments at freeze-out time can be used to distinguish the two collision configurations. Fig. 4 represents the differences between deformed and spherical ^{24}Mg + ^{24}Mg collisions. It can be seen from Fig. 4 that spherical collisions have more fragments till very large impact parameters. Specifically, the differences can be seen more obviously from the multiplicity of different kinds of fragments shown in Fig. 5. The spherical collisions have more light fragments and intermediate mass fragments (IMF) than deformed collisions while the heavy fragments are much fewer.

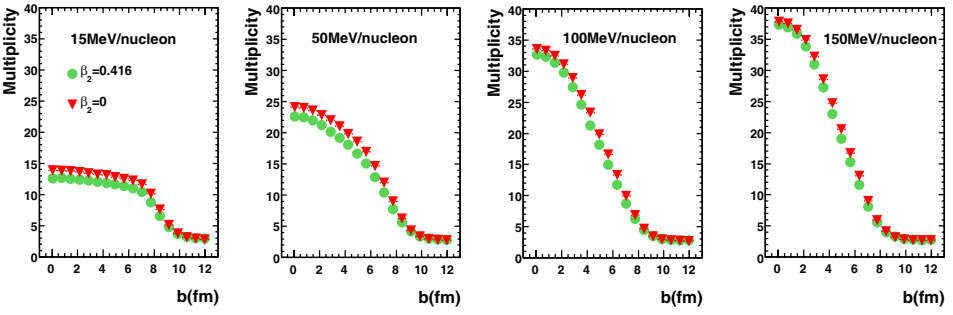

Fig. 4. (Color online) Multiplicity of fragments as a function of impact parameter at freeze-out time for deformed and spherical ^{24}Mg + ^{24}Mg collisions.

4. Summary

In summary, deformed ^{24}Mg + ^{24}Mg collisions have been studied by IDQMD model. Averaging all the collision orientations, the NN collision number, nuclear stopping power and fragments observables have non-ignorable effects compared with spherical ^{24}Mg + ^{24}Mg collisions, especially for the multiplicity of different kinds of fragments. Moreover, Orientation-average deformed nuclei collisions may have some implications on halo and cluster structure research.

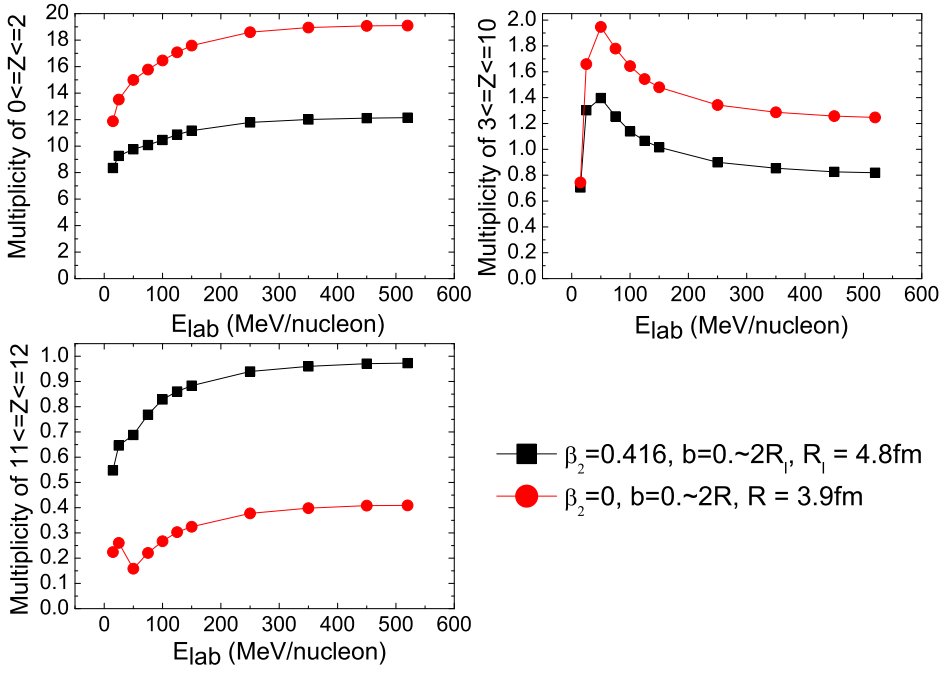

Fig. 5. (Color online) Multiplicity of light ($Z < 3$), intermediate mass ($3 \leq Z \leq 10$) and heavy ($11 \leq Z \leq 12$) fragments as a function of incident energy at freeze-out time for deformed and spherical ^{24}Mg + ^{24}Mg collisions.

Acknowledgments

This work is supported in part by National Natural Science Foundation of China under contract Nos. 10775167, 10775168, 10979074, 10605036, 10875160, 10805067 and 10975174, Major State Basic Research Development Program in China under contract No. 2007CB815004, the Shanghai Development Foundation for Science and Technology under contract No. 09JC1416800 and the National Defence Innovation Foundation of Chinese Academy of Science under grants No. CXJJ-216.

References

1. H. Marshak et al., *Phys. Rev. Lett.* **20**, (1968) 554.
2. D. R. Parks et al., *Phys. Rev. Lett.* **29**, (1972) 1264.
3. J. A. Christley and J. A. Tostevin, *Phys. Rev. C* **59**, (1999) 2309.
4. P. Filip, *Phys. At. Nucl.* **71**, (2008) 1609.
5. R. G. Stokstad et al., *Phys. Rev. Lett.* **41**, (1978) 465.
6. V. Y. Denisov and N. A. Pilipenko, *Phys. Rev. C* **76**, (2007) 014602.
7. S. Das Gupta and C. Gale, *Phys. Rev. C* **62**, (2000) 031901(R).
8. B. A. Li, *Phys. Rev. C* **61**, (2000) 021903(R).
9. E. V. Shuryak, *Phys. Rev. C* **61**, (2000) 034905.
10. U. Heinz and A. Kuhlman, *Phys. Rev. Lett.* **94**, (2005) 132301.

11. A. Kuhlman and U. Heinz, *Phys. Rev. C* **72**, (2005) 037901.
12. C. Nepali, G. Fai, and D. Keane, *Phys. Rev. C* **76**, (2007) 051902(R).
13. X. F. Luo et al., *Phys. Rev. C* **76**, (2007) 044902.
14. H. Masui et al., *Phys. Lett. B* **679**, (2009) 440.
15. D. Q. Fang et al., *Phys. Rev. C* **76**, (2007) 031601(R).
16. M. Freer, *Rep. Prog. Phys.* **70**, (2007) 2149.
17. G. A. Lalazissis et al., At. Data Nucl. Data Tables 71, (1999) 1.
18. J. Aichelin et al., *Phys. Rev. Lett.* **58**, (1987) 1926.
19. J. Aichelin, *Phys. Rep.* **202**, (1991) 233.
20. Y. B. Wei et al., *Phys. Lett. B* **586**, (2004) 225.
21. Y. G. Ma et al., *Phys. Rev. C* **73** (2006) 014604.
22. T. Z. Yan et al., *Phys. Lett. B* **638**, (2006) 50.
23. H. Ströbele et al., *Phys. Rev. C* **27**, (1983) 1349.